Supporting Information

Conformational distortion-harnessed singlet fission dynamics in Thienoquinoid: Rapid generation and subsequent annihilation of multiexciton dark State

Long Wang,[1] Teng-Shuo Zhang,[2,3] Xiangbin Tian,[1] Shaoting Guo,[1] Hua Wang,[1] Ganglong Cui,[3] Wei-Hai Fang,[3] Hongbing Fu,[4] and Jiannian Yao[5]*

[1]Key Laboratory of Interface Science and Engineering in Advanced Materials, Ministry of Education, Taiyuan University of Technology, Taiyuan 030024, China

[2] State Key Laboratory Breeding Base of Green Chemistry-Synthesis Technology, College of Chemical Engineering, Zhejiang University of Technology, Hangzhou, Zhejiang 310014, P. R. China

[3]Key Laboratory of Theoretical and Computational Photochemistry, Ministry of Education, College of Chemistry, Beijing Normal University, Beijing 100875, China

[4]Beijing Key Laboratory for Optical Materials and Photonic Devices, Department of Chemistry, Capital Normal University, Beijing 100048, China

[5]Beijing National Laboratory for Molecules Science (BNLMS), Key Laboratory of Photochemistry, Institute of Chemistry, Chinese Academy of Sciences, Beijing 100190, China

Table of Contents

1. Materials and Method.

1.1 Molecular Synthesis and Structural Characterization. TQ molecules were synthesized according to previous reported routes with some modifications.[1] Anthracene and other organic reagents were purchased from Innochem or J&K Chemicals. All solvents and reagents of the best grade available were purchased from commercial suppliers and used without further purification. NMR spectra were recorded on a Bruker Avance 400 spectrometer using the solvent peak as the reference standard, with chemical shifts given in parts per million. Tetrahydrofuran-d8 was used as NMR solvent. MALDI-TOF mass spectra were recorded on Bruker Ultra frex. X-ray diffraction (XRD) was carried out in the reflection mode at room temperature using a 2 kW Rigaku XRD system.

2,5-di(9H-fluoren-9-ylidene)-2,5-dihydrothiophene (**TQ**): dark green crystalline. ^{1}H NMR (400 MHz, C_4D_8O) δ: 8.43-8.44 (m, 2H), 8.29-8.31 (m, 2H), 8.17-8.20 (m, 2H), 7.83-7.87 (m, 4H), 7.47-7.51 (m, 2H), 7.35-7.43 (m, 6H). HRMS (ESI-TOF) Calculated for $C_{30}H_{18}S$: 410.1129, found: m/z 410.1124.

1.2 Sample Preparation. TQ-doped polymethyl methacrylate (PMMA) films (weight ratio of 5%) were prepared by spin-coating method on sapphire substrate at 3000 r.p.m. for 1 min in a nitrogen-filled glove box. Neat films were prepared by vapor deposition method on sapphire substrate at a rate of 0.3 Å/s under a vacuum of 1×10^{-5} mbar.

1.3 Spectroscopic Measurement and Analysis. UV-visible absorption and fluorescence spectra were measured on Shimadzu UV-3600 spectrometer and Hitachi F-4500 spectrophotometer, respectively. All the spectra were measured at room temperature if no further notification. Femtosecond transient absorption (fs-TA) and nanosecond transient absorption (ns-TA) spectroscopy measurements were all performed using previously described instruments and experimental conditions.[2-3]

2. Thin Film Characterization.

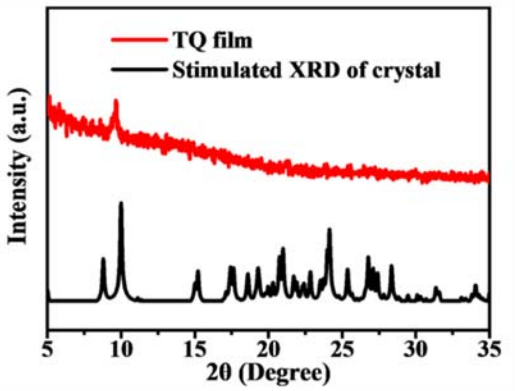

Figure S1. XRD diffractograms (red) and simulated powder patterns (black) of **TQ** film. Results show that the neat film is polycrystalline and features similar intermolecular interactions observed in the respective single crystal structure.

3. Theoretical Calculations.

All geometry optimizations are calculated with state-averaged CASSCF (SA-CASSCF) and all reported energies are evaluated by CASPT2.[4-5] CASPT2//CASSCF is one of the few electronic structure methods capable of treating singlet fission because it involves clear double-excitation problems. In all the CASPT2//CASSCF calculations, an active space of 12 electrons in 12 orbitals is used to obtain accurate results. The ANO-RCC-VDZP basis set is adopted in the geometry optimizations and in the single-point energy calculations.[6] The imaginary shift technique (0.2 au) is used to avoid the intruder-state issues and the ionization potential electron affinity shift is set to zero according to recent benchmarks.[7-8] In geometry optimizations, state-averaged CASSCF calculations with five roots (equal weights) are used. Finally, single-point energies are calculated at the CASPT2 level on the basis of state-averaged CASSCF calculation. The Cholesky decomposition technique with unbiased auxiliary basis sets is used for accurate two-electron integral approximation.[9] All the CASPT2//CASSCF calculations are carried out with the OpenMolcas package.[10]

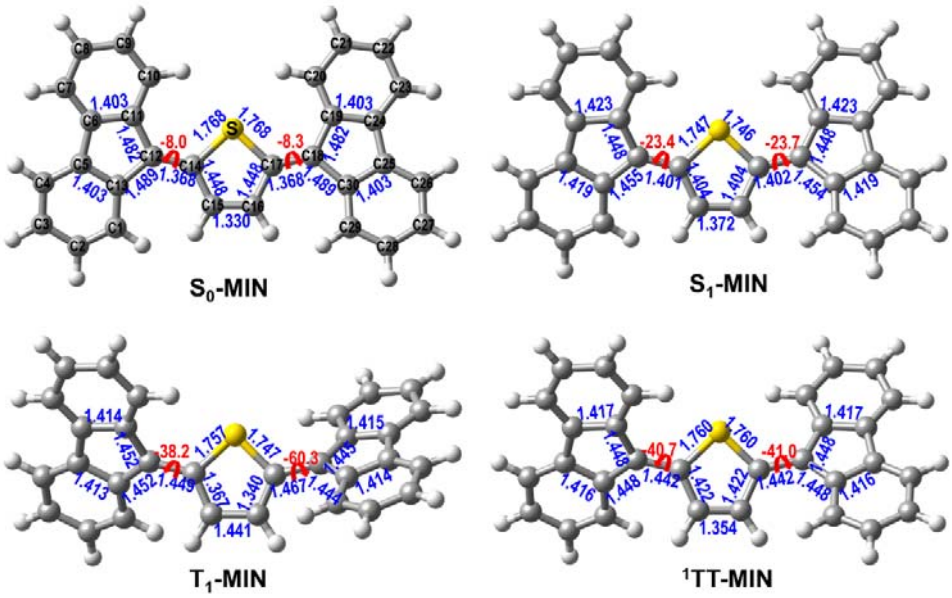

Figure S2. CAS(12,12) optimized excited-state minimum-energy structures, also shown are selected bond-length.

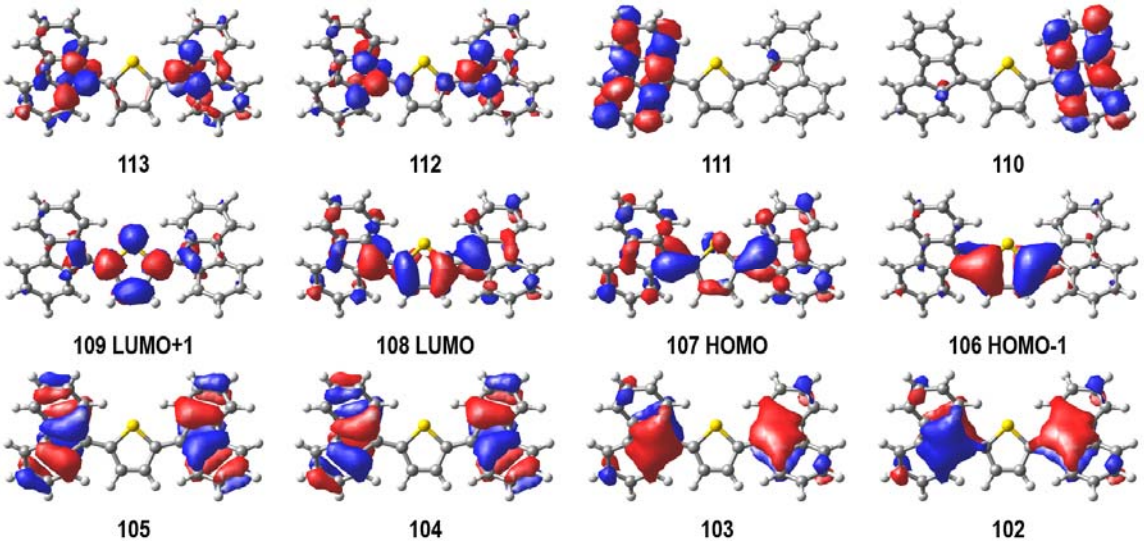

Figure S3. Molecular orbitals used as the active space of 12 electrons in 12 orbitals in all CASPT2//CASSCF calculations.

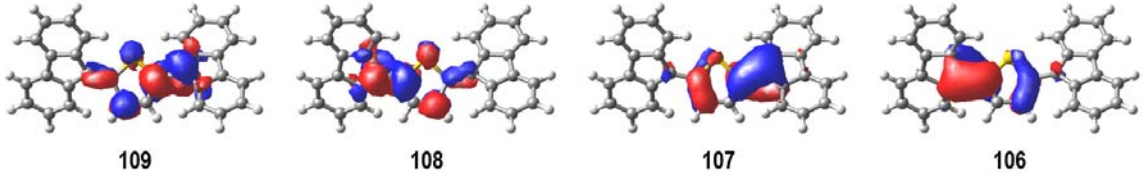

Figure S4. Localized molecular orbitals used in the active space of 12 electrons in 12 orbitals, note, other orbitals remain the same as original.

Table S1. CASPT2//CASSCF/ANO-RCC-VDZP computed absolute energies (A.E. in au), relative energies (ΔE), electronic configurations, and associated weights at the different minimum-energy structures.

State	Root	A.E.	ΔE		Configurations	Weights
			kcal·mol^{-1}	eV		
S_0 (1^1A)-MIN	**1**	-1550.06355	**0.0**	**0.0**	**222222000000**	**0.80**
	2	-1549.97790	53.7	2.33	22222ud00000	0.78
	3	-1549.96373	62.6	2.71	2222u2d00000 222u2d200000	0.56 0.15
	4	-1549.96219	63.6	2.76	222u22d00000 2222ud200000	0.58 0.16
	5	-1549.97790	64.9	2.81	222220200000 22u222d00000 22222u0d0000	0.34 0.21 0.17
S_1 (1^1B)-MIN	1	-1550.06264	0.6	0.03	222222000000	0.74
	2	-1549.99065	**45.7**	**1.98**	**22222ud00000**	**0.80**
	3	-1549.98839	47.2	2.05	222220200000 22u222d00000 22222u0d0000	0.37 0.20 0.16
	4	-1549.97442	55.9	2.42	2222u2d00000 222u2d200000	0.48 0.15
	5	-1549.97398	56.2	2.44	222u22d00000 2222ud200000	0.48 0.15
TT (2^1A)-MIN	1	-1550.05172	7.4	0.32	222222000000 222220200000	0.65 0.14
	2	**-1549.99389**	**43.7**	**1.90**	**222220200000** **22u222d00000** **22222u0d0000**	**0.30** **0.19** **0.18**
	3	-1549.98821	47.3	2.05	22222ud00000	0.78
	4	-1549.97094	58.1	2.52	2222u2d00000 2222ud200000 222u22d00000	0.28 0.25 0.14
	5	-1549.97089	58.1	2.52	222u22d00000 222u2d200000 2222u2d00000	0.28 0.25 0.14
T_1 (1^3B)-MIN	1	-1550.03429	18.4	0.80	22222uu00000	0.79
P1-MIN	1	-1549.91899	90.6	3.93	2222uuuu0000	0.81

Table S2. Hole and particle state-averaged natural transition orbitals involved in the transitions of S_1, TT, and T_1 states.

S_1 state	Hole	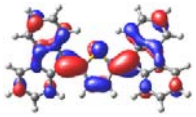	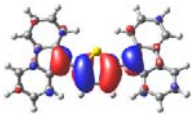
		h_1	h_2
	Particle	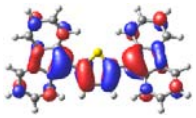	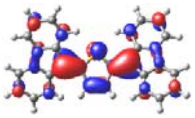
		e_1	e_2
	Weight %	89.9	8.6
TT state	Hole		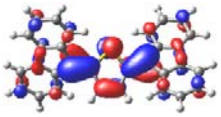
		h_1	h_2
	Particle	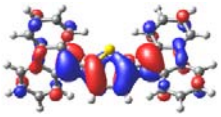	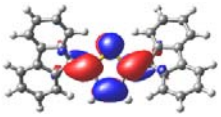
		e_1	e_2
	Weight %	53.2	45.3
T_1 state	Hole (Alpha Spin)		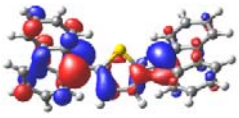
		h_1	h_2
	Particle (Alpha Spin)		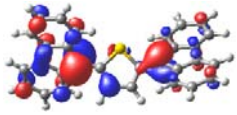
		e_1	e_2
	Weight %	57.5	40.0
	Hole (Beta Spin)	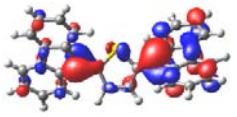	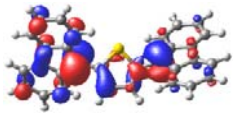
		h_1	h_2
	Particle (Beta Spin)		
		e_1	e_2
	Weight %	57.5	40.0

4. Triplet Sensitization in Solution.

The triplet ESA signature, and its energy level, E(T_1), of **TQ** were determined by a triplet-triplet energy-transfer method. Determination performed in an air-free solution containing relatively high concentration of triplet sensitizer **Anthracene** (**An**), which can yield at ultrafast rate the triplet state via ISC process after pulse radiolysis and then transfer it to the target molecule. Upon 355 nm-excitation, the long-lived triplet signal (^{3}**An***) are clearly observed around 400-430 nm in the mixed **An**/**TQ** solution. Then the initially populated ^{3}**An*** can be quenched via triplet-triplet energy transfer process, and triplet signal of **TQ** (^{3}**TQ***) appears at long wavelength. It should be noted that laser irradiation of the dilute solution of **TQ** itself at 355 nm results in undetectable long-lived transient signals in the ns-to-µs time range. These results rule out the possibility of triplet generation via conventional ISC process.

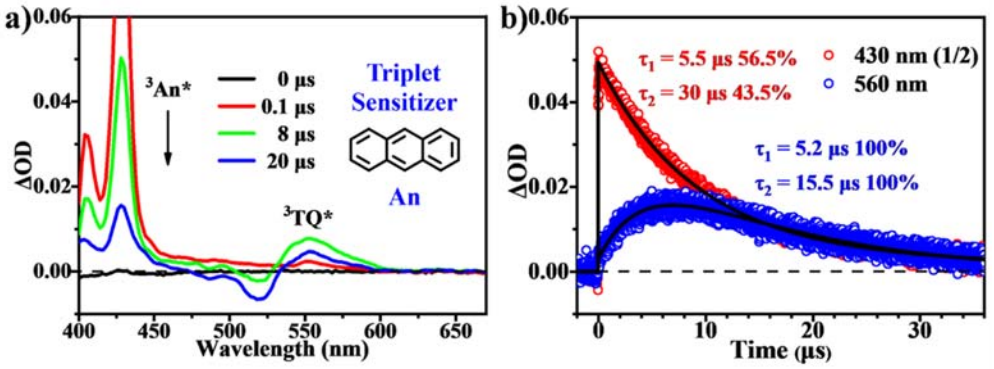

Figure S5. ns-TA spectra and corresponding kinetic traces for **Anthracene**/**TQ** solution upon 355 nm excitation.

5. Dependence on Excitation Energy in TA measurements.

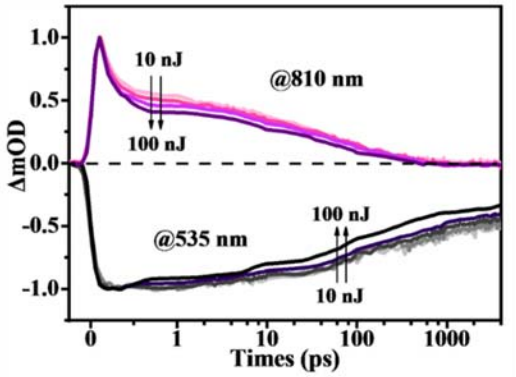

Figure S6. Normalized kinetic profiles for thin film upon excitation at 470 nm with different excitation energies (10, 20, 30, 50, and 100 nJ). Results show that at the lower excitation energies of 10, 20, and 30 nJ, the kinetics exhibit almost identical decay trends indicating similar SF dynamics. At the higher excitation energies of 50, and 100 nJ, the kinetics show the more rapid decay trends, which are then attributed to the presence of singlet-singlet annihilation process after photoexcitation. Therefore, we used the excitation energy of 20 nJ in the fs-TA measurements for neat films.

6. Triplet Sensitization in Solid Film.

Triplet sensitization in solid-state was performed by blending a small portion (~ 10 mol%) of $PdPc(OBu)_8$ (**PP8**) into PMMA or **TQ** thin film.[11-13] The fs-TA measurements were performed by selectively exciting the **PP8** molecules in PMMA film or **TQ** doped thin films at 740 nm.

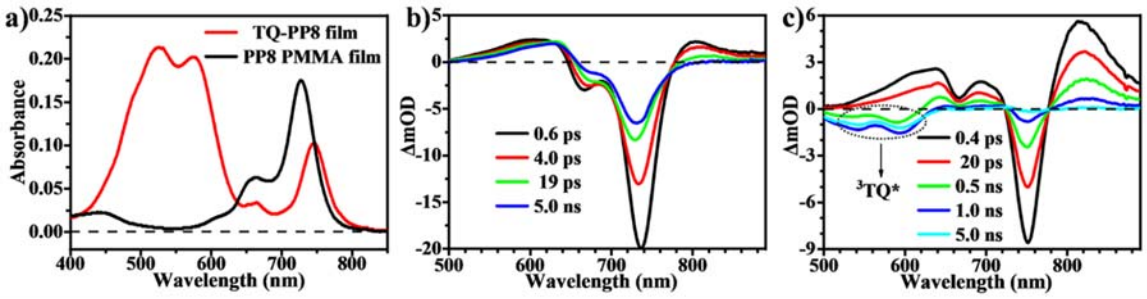

Figure S7. a) Steady state absorption spectra of sensitizer **PP8** PMMA film and **TQ-PP8** doped films. b, c) fs-TA spectra of **PP8** PMMA film and **TQ-PP8** doped films (excitation at 740 nm, where **TQ** molecules show negligible absorbance).

7. Heating Effect in Neat Film.

Rao *et al.* observed that laser heating have significant effects on fs-TA spectra and kinetics in thin film samples of semiconducting polymers and SF materials and these heating artifacts can persist for tens of nanoseconds.[14-15] We have performed control experiments using the methods reported by Nichols *et al.*[16] Results show that these noise signals turn out to have little contribution to fs-TA data in neat films of current system.

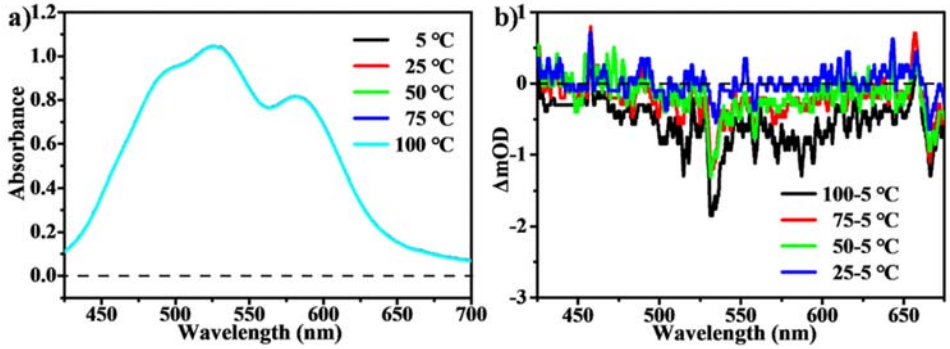

Figure S8. a) Steady state absorption spectra of a 50 nm thick **TQ** neat film at temperatures ranging from 5 to 100 ℃. b) Difference spectrum between higher temperature (100, 75, 50, and 25 ℃) and 5 ℃ absorption spectra.

8. References.

1. Kawata, S.; Pu, Y. J.; Saito, A.; Kurashige, Y.; Beppu, T.; Katagiri, H.; Hada, M.; Kido, J., Singlet Fission of Non-Polycyclic Aromatic Molecules in Organic Photovoltaics. *Adv. Mater*. **2016,** *28*, 1585-1590.

2. Wang, L.; Lin, L.; Yang, J.; Wu, Y.; Wang, H.; Zhu, J.; Yao, J.; Fu, H., Singlet Fission in a Pyrrole-Fused Cross-Conjugated Skeleton with Adaptive Aromaticity. *J. Am. Chem. Soc.* **2020,** *142*, 10235-10239.

3. Wang, L.; Zhang, T.-S.; Fu, L.; Xie, S.; Wu, Y.; Cui, G.; Fang, W.-H.; Yao, J.; Fu, H., High-Lying 3^1A_g Dark-State-Mediated Singlet Fission. *J. Am. Chem. Soc.* **2021,** *143*, 5691-5697.

4. Andersson, K.; Malmqvist, P. Å.; Roos, B. O., Second-Order Perturbation Theory with a Complete Active Space Self-Consistent Field Reference Function. *J. Chem. Phys.* **1992,** *96*, 1218-1226.

5. Andersson, K.; Malmqvist, P. A.; Roos, B. O.; Sadlej, A. J.; Wolinski, K., Second-Order Perturbation Theory with a CASSCF Reference Function. *J. Phys. Chem.* **1990,** *94*, 5483-5488.

6. Roos, B. O.; Lindh, R.; Malmqvist, P. A.; Veryazov, V.; Widmark, P. O., Main Group Atoms and Dimers Studied with a New Relativistic Ano Basis Set. *J. Phys. Chem. A* **2004,** *108*, 2851-2858.

7. Ghigo, G.; Roos, B. O.; Malmqvist, P.-Å., A Modified Definition of the Zeroth-Order Hamiltonian in Multiconfigurational Perturbation Theory (CASPT2). *Chem. Phys. Lett.* **2004,** *396*, 142-149.

8. Zobel, J. P.; Nogueira, J. J.; González, L., The IPEA Dilemma in CASPT2. *Chem. Sci.* **2017,** *8*, 1482-1499.

9. Aquilante, F.; Lindh, R.; Pedersen, T. B., Unbiased Auxiliary Basis Sets for Accurate Two-Electron Integral Approximations. *J. Chem. Phys.* **2007,** *127*.

10. Aquilante, F.; Autschbach, J.; Baiardi, A.; Battaglia, S.; Borin, V. A.; Chibotaru, L. F.; Conti, I.; De Vico, L.; Delcey, M.; Galvan, I. F.; Ferre, N.; Freitag, L.; Garavelli, M.; Gong, X.; Knecht, S.; Larsson, E. D.; Lindh, R.; Lundberg, M.; Malmqvist, P. A.; Nenov, A.; Norell, J.; Odelius, M.; Olivucci, M.; Pedersen, T. B.; Pedraza-Gonzalez, L.; Phung, Q. M.; Pierloot, K.; Reiher, M.; Schapiro, I.; Segarra-Marti, J.; Segatta, F.; Seijo, L.; Sen, S.; Sergentu, D.-C.; Stein, C. J.; Ungur, L.; Vacher, M.; Valentini, A.; Veryazov, V., Modern Quantum Chemistry with Open Molcas. *J. Chem. Phys.* **2020,** *152*.

11. Hartnett, P. E.; Margulies, E. A.; Mauck, C. M.; Miller, S. A.; Wu, Y.; Wu, Y.-L.; Marks, T. J.; Wasielewski, M. R., Effects of Crystal Morphology on Singlet Exciton Fission in Diketopyrrolopyrrole Thin Films. *J. Phys. Chem. B* **2016,** *120*, 1357-1366.

12. Korovina, N. V.; Das, S.; Nett, Z.; Feng, X.; Joy, J.; Haiges, R.; Krylov, A. I.; Bradforth, S. E.; Thompson, M. E., Singlet Fission in a Covalently Linked Cofacial Alkynyltetracene Dimer. *J. Am. Chem. Soc.* **2016,** *138*, 617-627.

13. Bae, Y. J.; Kang, G.; Malliakas, C. D.; Nelson, J. N.; Zhou, J.; Young, R. M.; Wu, Y.-L.; Van Duyne, R. P.; Schatz, G. C.; Wasielewski, M. R., Singlet Fission in 9,10-Bis(Phenylethynyl)Anthracene Thin Films. *J. Am. Chem. Soc.* **2018,** *140*, 15140-15144.

14. Albert-Seifried, S.; Friend, R. H., Measurement of Thermal Modulation of Optical Absorption in Pump-Probe Spectroscopy of Semiconducting Polymers. *Appl. Phys. Lett.* **2011,** *98*, 223304.

15. Rao, A.; Wilson, M. W. B.; Albert-Seifried, S.; Di Pietro, R.; Friend, R. H., Photophysics of Pentacene Thin Films: The Role of Exciton Fission and Heating Effects. *Phys. Rev. B* **2011,** *84*, 195411.

16. Nichols, V. M.; Broch, K.; Schreiber, F.; Bardeen, C. J., Excited-State Dynamics of Diindenoperylene in Liquid Solution and in Solid Films. *J. Phys. Chem. C* **2015,** *119*, 12856-12864.

9. Appendix.

9.1 NMR Spectra.

Figure S9. ^{1}H NMR spectra of **TQ** in C_4D_8O.

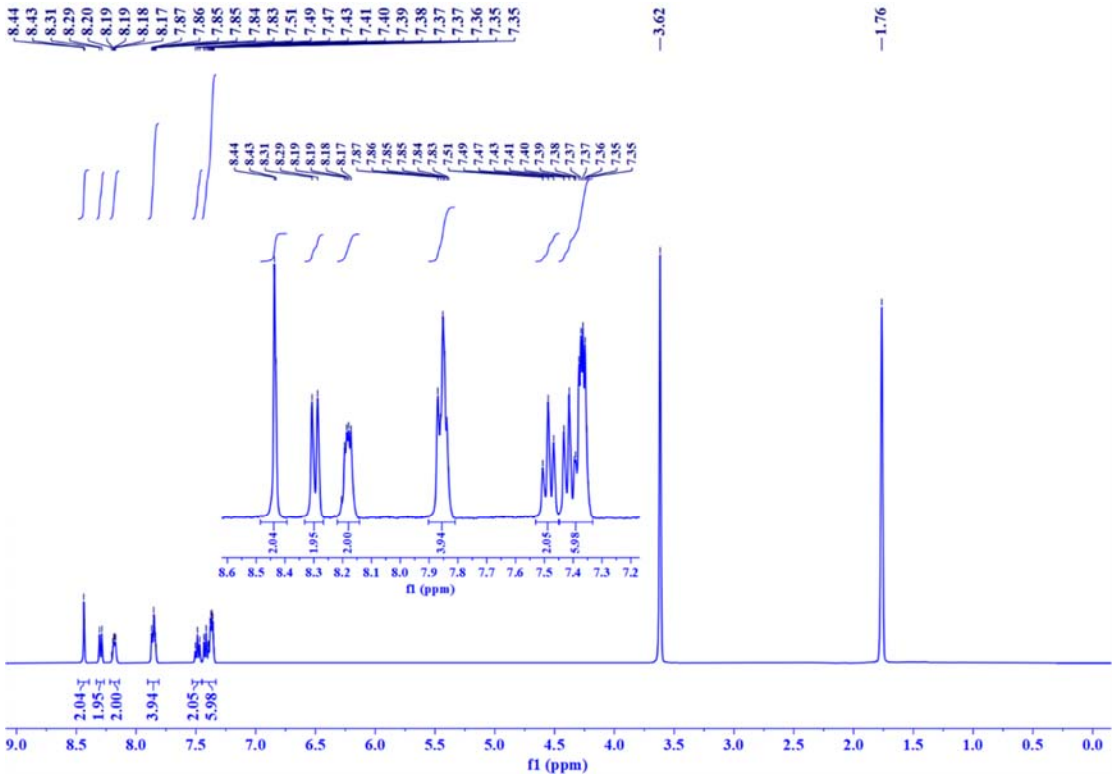

9.2 Cartesian Coordinates of All Optimized Structures (in Angstrom).

S_0 (1^1A) minimum-energy point				**S_1 (1^1B) minimum-energy point**			
C	0.034948	0.981834	0.043699	C	0.080827	0.900863	0.134306
C	-0.606686	1.399524	1.272351	C	-0.558777	1.367863	1.315000
C	-1.658702	0.677612	1.648792	C	-1.708130	0.722854	1.624763
C	-2.024552	-0.408290	0.764199	C	-2.075854	-0.300981	0.709438
S	-0.867545	-0.407996	-0.572488	S	-0.868876	-0.404233	-0.567048
C	1.141561	1.517444	-0.555688	C	1.275019	1.417684	-0.487140
C	-3.069291	-1.282358	0.887658	C	-3.200580	-1.199387	0.793656
C	1.881475	2.746264	-0.156740	C	1.654054	2.813147	-0.554700

C	3.011661	2.878392	-0.977421	C	2.900100	2.919910	-1.219316
C	3.022638	1.772000	-1.940508	C	3.321963	1.560872	-1.591960
C	1.893971	0.971114	-1.709997	C	2.321254	0.663309	-1.145143
C	-4.007399	-1.414259	2.036052	C	-3.726300	-1.780476	2.010800
C	-4.990623	-2.359987	1.708760	C	-4.844417	-2.588099	1.689566
C	-4.706342	-2.886064	0.369236	C	-5.031837	-2.526664	0.231820
C	-3.544805	-2.265340	-0.114559	C	-4.022208	-1.684504	-0.295428
C	1.627951	3.749422	0.785252	C	0.999395	3.975600	-0.131686
C	2.505847	4.802677	0.915950	C	1.598729	5.198639	-0.346379
C	3.637550	4.898423	0.115820	C	2.830467	5.288491	-0.981205
C	3.886922	3.934174	-0.843748	C	3.484147	4.138821	-1.427346
C	3.924704	1.479723	-2.937196	C	4.441316	1.106029	-2.232050
C	3.709300	0.366382	-3.733444	C	4.591689	-0.265805	-2.441149
C	2.599474	-0.438326	-3.518099	C	3.624273	-1.156763	-1.997101
C	1.694226	-0.152072	-2.517839	C	2.492523	-0.711064	-1.347060
C	-5.385833	-3.825109	-0.371726	C	-5.963749	-3.105252	-0.584538
C	-4.907278	-4.165924	-1.626638	C	-5.912046	-2.853477	-1.956438
C	-3.761294	-3.560123	-2.122017	C	-4.935367	-2.019903	-2.483938
C	-3.078572	-2.615291	-1.385054	C	-3.991914	-1.427537	-1.670931
C	-4.036806	-0.845343	3.314078	C	-3.296442	-1.699614	3.340240
C	-5.043383	-1.184880	4.190807	C	-3.991523	-2.386905	4.312651
C	-6.027757	-2.098680	3.835617	C	-5.098613	-3.159543	3.987509
C	-5.995397	-2.697302	2.589258	C	-5.525160	-3.266003	2.662850
H	-0.244242	2.212919	1.858843	H	-0.139813	2.154190	1.911102
H	-2.213933	0.909581	2.529128	H	-2.314834	0.965185	2.474713
H	0.755171	3.745409	1.402380	H	0.037167	3.928316	0.341161
H	2.303722	5.567431	1.644289	H	1.102757	6.096290	-0.023309

H	4.308665	5.729825	0.232949	H	3.279890	6.252045	-1.139212
H	4.748092	4.016532	-1.481514	H	4.429761	4.221931	-1.932223
H	4.786275	2.101329	-3.099979	H	5.202069	1.786493	-2.570090
H	4.403153	0.123708	-4.517801	H	5.466244	-0.635157	-2.945286
H	2.440859	-1.301910	-4.138631	H	3.760441	-2.210869	-2.159470
H	0.858051	-0.805312	-2.385033	H	1.761356	-1.417046	-1.003198
H	-6.275982	-4.290097	0.011188	H	-6.731413	-3.743341	-0.185059
H	-5.424811	-4.898727	-2.218836	H	-6.637834	-3.304470	-2.608558
H	-3.398032	-3.828128	-3.097830	H	-4.915690	-1.830452	-3.542128
H	-2.204682	-2.170145	-1.811390	H	-3.251195	-0.778697	-2.097133
H	-3.285261	-0.164932	3.653110	H	-2.430453	-1.125108	3.608129
H	-5.059035	-0.740664	5.169893	H	-3.668409	-2.329038	5.336561
H	-6.803214	-2.351139	4.535813	H	-5.625825	-3.687916	4.760981
H	-6.740394	-3.423319	2.319027	H	-6.373815	-3.880222	2.420949

ME (2^1A) minimum-energy point				**T_1 (1^3B) minimum-energy point**			
C	0.055995	0.950673	0.127103	C	0.001593	1.000271	0.116944
C	-0.568273	1.396243	1.303574	C	-0.710458	1.588555	1.124114
C	-1.703919	0.706990	1.646303	C	-1.924600	0.886743	1.454651
C	-2.058335	-0.319442	0.756128	C	-2.130342	-0.206052	0.707561
S	-0.874668	-0.374914	-0.526709	S	-0.836723	-0.439266	-0.442764
C	1.209143	1.450494	-0.492823	C	1.247849	1.448822	-0.471376
C	-3.140510	-1.206834	0.832563	C	-3.248018	-1.153130	0.787148
C	1.765679	2.781609	-0.306888	C	1.629348	2.833407	-0.685164
C	2.952569	2.896038	-1.076525	C	2.923091	2.869194	-1.253282
C	3.154759	1.627237	-1.775088	C	3.381946	1.479821	-1.407384
C	2.082710	0.761251	-1.419777	C	2.354077	0.630833	-0.935567

C	-3.873306	-1.551722	2.040533	C	-3.615846	-1.931028	1.947165
C	-4.915939	-2.454288	1.704708	C	-4.745649	-2.719804	1.629127
C	-4.845078	-2.700962	0.265006	C	-5.105267	-2.435623	0.228951
C	-3.755564	-1.944435	-0.251075	C	-4.182272	-1.484060	-0.264492
C	1.314698	3.903418	0.397698	C	0.938730	4.030533	-0.476562
C	2.058185	5.072164	0.367372	C	1.549820	5.223710	-0.802417
C	3.229032	5.155552	-0.360253	C	2.828062	5.247009	-1.342054
C	3.675108	4.054976	-1.099583	C	3.519030	4.058198	-1.576119
C	4.143761	1.220803	-2.623043	C	4.557782	0.967633	-1.885229
C	4.105341	-0.074888	-3.151003	C	4.736302	-0.415125	-1.900774
C	3.082697	-0.937012	-2.801969	C	3.740159	-1.258584	-1.428759
C	2.075486	-0.542387	-1.939616	C	2.553236	-0.753565	-0.940733
C	-5.619471	-3.475308	-0.549333	C	-6.111786	-2.911797	-0.567828
C	-5.339487	-3.523330	-1.919872	C	-6.215422	-2.443441	-1.877475
C	-4.298107	-2.779451	-2.442553	C	-5.315852	-1.503982	-2.368026
C	-3.506928	-1.985430	-1.631771	C	-4.300510	-1.014851	-1.576681
C	-3.684485	-1.218466	3.386543	C	-3.044225	-2.013215	3.220523
C	-4.543674	-1.733632	4.343587	C	-3.606836	-2.861454	4.147681
C	-5.574053	-2.584655	3.994946	C	-4.721354	-3.629843	3.829514
C	-5.754629	-2.956784	2.658598	C	-5.294603	-3.560878	2.559869
H	-0.163011	2.179428	1.907152	H	-0.382897	2.469798	1.638409
H	-2.299326	0.959598	2.497051	H	-2.602564	1.208859	2.221858
H	0.392148	3.894305	0.941177	H	-0.059071	4.032306	-0.082267
H	1.709529	5.929653	0.914603	H	1.025335	6.148694	-0.642254
H	3.791246	6.071377	-0.372405	H	3.285372	6.187492	-1.590876
H	4.573887	4.132830	-1.684534	H	4.502351	4.085749	-2.010083
H	4.950603	1.880998	-2.885762	H	5.339552	1.613990	-2.241719

H	4.878516	-0.401515	-3.822151	H	5.654443	-0.830328	-2.275191
H	3.068912	-1.935070	-3.201578	H	3.897270	-2.322244	-1.439593
H	1.314433	-1.249215	-1.679197	H	1.802653	-1.423588	-0.568722
H	-6.441194	-4.043312	-0.151788	H	-6.817695	-3.634244	-0.199083
H	-5.942524	-4.133315	-2.567324	H	-7.000620	-2.810894	-2.513111
H	-4.099493	-2.811493	-3.498745	H	-5.416540	-1.153697	-3.379665
H	-2.724682	-1.408416	-2.081099	H	-3.611770	-0.287005	-1.963510
H	-2.874188	-0.594633	3.704234	H	-2.178813	-1.427623	3.470135
H	-4.397142	-1.470420	5.375853	H	-3.178005	-2.934601	5.131108
H	-6.229373	-2.974987	4.752023	H	-5.143383	-4.286501	4.568616
H	-6.542715	-3.639315	2.395679	H	-6.152516	-4.165190	2.325359

P1 minimum-energy point

C	0.157370	0.768218	0.216660
C	-0.557099	1.322731	1.388458
C	-1.767969	0.833770	1.572657
C	-2.198244	-0.145016	0.547199
S	-0.890372	-0.396517	-0.653904
C	1.360237	1.323590	-0.398969
C	-3.308035	-1.086909	0.676633
C	1.428584	2.464189	-1.285610
C	2.776421	2.679919	-1.653881
C	3.589437	1.645409	-0.986432
C	2.708042	0.833927	-0.233809
C	-3.318695	-2.311847	1.445736
C	-4.585898	-2.925046	1.315480
C	-5.404402	-2.069268	0.435553

C	-4.606845	-0.962829	0.059326
C	0.425739	3.303115	-1.776895
C	0.777150	4.334348	-2.619831
C	2.103702	4.540446	-2.979030
C	3.112659	3.707495	-2.492510
C	4.933042	1.390657	-0.994932
C	5.422593	0.316300	-0.248588
C	4.561555	-0.486294	0.491144
C	3.206641	-0.240961	0.506896
C	-6.689531	-2.186155	-0.017127
C	-7.203514	-1.195720	-0.857300
C	-6.424205	-0.107413	-1.232803
C	-5.128401	0.021080	-0.784871
C	-2.329528	-2.909032	2.230402
C	-2.614451	-4.096996	2.866840
C	-3.861586	-4.695415	2.733701
C	-4.856511	-4.105524	1.952359
H	-0.087412	2.050149	2.022859
H	-2.424291	1.109576	2.375961
H	-0.602290	3.143674	-1.507458
H	0.016677	4.986595	-3.009935
H	2.356005	5.349435	-3.640233
H	4.134056	3.878808	-2.781406
H	5.612262	2.002745	-1.560667
H	6.477123	0.108500	-0.246112
H	4.961127	-1.308064	1.057665
H	2.544506	-0.864283	1.079879

H	-7.305651	-3.020794	0.265398
H	-8.213246	-1.276090	-1.216744
H	-6.841063	0.642553	-1.880642
H	-4.529503	0.864191	-1.077726
H	-1.361332	-2.453779	2.331103
H	-1.862427	-4.571695	3.471039
H	-4.062290	-5.623880	3.236672
H	-5.815776	-4.581888	1.857767